doi.org/10.36721/PJPS.2026.39.9.269.1

Unraveling the regulatory mechanisms of tetrandrine in microglial phenotypic transition and neuronal autophagy for relieving diabetic neuropathic pain

QiaoZhen Liu and Hua Zhang*
Department of Anesthesiology and Pain Management, The Third People's Hospital of Hangzhou, Hangzhou City, Zhejiang Province, 310009, China

Abstract: **Background**: Diabetic neuropathic pain (DNP) is a prevalent and debilitating complication of diabetes mellitus, characterized by persistent pain and neuroinflammation. Current treatments often provide inadequate relief, highlighting the need for novel therapeutic strategies targeting its underlying mechanisms. **Objectives**: This study aimed to investigate the therapeutic potential of tetrandrine (Tet) in alleviating DNP and to elucidate its effects on two key pathological processes: neuronal autophagy and microglial polarization. **Methods**: To establish the DNP model, rats received an intraperitoneal injection of streptozotocin. Pain behavior was assessed weekly using mechanical withdrawal threshold and thermal withdrawal latency tests. Relevant markers were analyzed via reverse-transcription quantitative real-time polymerase chain reaction, enzyme-linked immunosorbent assay, immunofluorescence, or Western blot. To further investigate the underlying mechanisms, *in-vitro* experiments were conducted using high glucose-treated neuronal cells and lipopolysaccharide-stimulated BV2 microglia. **Results**: Tet administration significantly alleviated pain hypersensitivity and neuroinflammation in DNP rats. Mechanistically, this effect might be achieved through a dual modulation of neuroimmune processes and intracellular clearance pathways. Tet shifted microglial polarization from the pro-inflammatory M1 phenotype toward the anti-inflammatory M2 state. Concurrently, it enhanced autophagic activity, as evidenced by an increased LC3-II level and LC3-II/LC3-I ratio, restored expression of the mitophagy-related proteins PINK1 and parkin and reduced p62 accumulation. *In-vitro* findings corroborated these mechanisms: Tet balanced the expression of M1 and M2 markers in activated microglia and similarly upregulated key autophagy-related proteins (LC3-II, PINK1, parkin) in neurons under high-glucose stress. **Conclusion**: Tet alleviates DNP, potentially through the concurrent modulation of microglial phenotypic transition and neuronal autophagy. These findings identify Tet as a promising multi-target agent for DNP and elucidate its potential mechanisms of action.

Keywords: Autophagy; Diabetic neuropathic pain; Mitochondria; Microglia; M1/M2; Tetrandrine

Submitted on 23-09-2025 – Revised on 04-01-2026 – Accepted on 17-01-2026

INTRODUCTION

Diabetes mellitus (DM) has become a major global public health issue, marked by a significant rise in its prevalence (Antar *et al*. 2023). A common complication of DM is diabetic neuropathic pain (DNP), which involves spontaneous nociceptive hypersensitivity, such as tingling and ants crawling sensations in symmetrical limbs (Li *et al*., 2023). DNP can lead to sleep disturbances, anxiety and depression, which can reduce patients' quality of life (R. Zhang *et al*. 2022; Gazzeri *et al*. 2025). The primary treatment strategy for DNP is to manage high blood glucose and other modifiable risk factors, although these efforts may not suffice to prevent or reduce DNP (Jang and Oh, 2023; Braffett *et al*., 2024). The present pharmacological approach to treating DNP includes opioids, antidepressants and topical agents like capsaicin and gamma-aminobutyric acid analogs (Bhandari *et al*., 2021). As the complex pathophysiology of DNP has not been fully elucidated, it is frequently underassessed and undertreated, leading to a small number of patients achieving satisfactory pain relief (Breitinger and Breitinger, 2023). Hence, the formulation of novel targeted therapeutic strategies for DNP is an immediate clinical concern.

Composed mainly of neurons and glial cells, the dorsal horn of the spinal cord is the primary entryway for peripheral sensory signals like nociception and itch to the central nervous system. Microglia activation has been found to be essential in the progression of neuropathic pain (Ding, 2025). Microglia activation, along with the ensuing spinal neuroinflammatory cascade are critical to DNP development. Following peripheral nerve injury, pain signals reach the dorsal root ganglia (DRGs) and the dorsal horn of the spinal cord via primary receptors, releasing neurotransmitters to activate microglia. When microglia are activated, they release proinflammatory cytokines that cause excitatory responses in spinal cord neurons, resulting in sensory neuropathies and pain, which contribute to central sensitization (Kuthati *et al*., 2023; Chong and Souayah, 2025). Activated microglia can be polarized to either the M1 or the M2 phenotype. M1 microglia are proinflammatory and cytotoxic, promoting

**Corresponding author:* e-mail: huazh581@outlook.com

neuroinflammation and exacerbating central sensitization, whereas M2 microglia are anti-inflammatory and neuroprotective, inhibiting neuroinflammation to reduce central sensitization. Therefore, strategies that prevent M1 polarization and encourage M2 polarization may be effective in treating DNP (Si *et al*., 2024).

Autophagy is a cellular degradation and recycling process that supports tissue homeostasis and energy supply (Klionsky *et al*., 2021; S. Liu *et al*., 2023). As long-lived, postmitotic cells, neurons particularly rely on autophagy to clear toxic or dysfunctional proteins and organelles, thereby maintaining neurotransmission and preserving the integrity of their functional proteome. This process exerts a protective effect on neuronal cells and is crucial for supporting neuroplasticity and normal nervous system function (Puglisi-Allegra *et al*. 2023; Karpova *et al*. 2025). Autophagy aids in restoring peripheral nerve function by promoting myelin and axonal regeneration, making targeted autophagy regulation a promising therapeutic strategy for peripheral nerve regeneration (Yon *et al*. 2023; Chen *et al*. 2025). The involvement of autophagy in neuropathic pain has been identified, with insufficient autophagic activity potentially leading to disease development (Zheng *et al*., 2023). Docosahexaenoic acid-rich supplements for type 2 DM patients reduce circulating neurotoxic lipids and raise serum ATG5, an autophagy marker (Durán *et al*., 2024). Moreover, bupivacaine induces defective autophagy, aggravating nociceptive hypersensitivity in DNP mice. Meanwhile, activating autophagy with rapamycin can decrease nociceptive hypersensitivity in bupivacaine-treated DNP mice, whereas inhibiting autophagy with bafilomycin A1 exacerbates it (Fan *et al*., 2024). This points to the possibility that restoring autophagy under local anesthesia and pain management could treat DNP.

Tetrandrine (Tet), a natural compound derived from the plant Stephania tetrandra S. Moore, exhibits a broad spectrum of pharmacological properties, including anticancer, antibacterial, anti-inflammatory, antioxidant, immunosuppressive, cardiovascular and calcium channel-blocking activities (Gong *et al*., 2024). Notably, Tet has been shown to significantly inhibit DM and associated kidney damage (L. Su *et al*., 2020), highlighting its therapeutic potential for DNP. Furthermore, Tet alleviates mechanical hyperalgesia in a spared nerve injury model in mice, an effect attributed to reduced neuroinflammation and decreased levels of chemokine-like factor 1 (Z.L. Zhang *et al*., 2023). While these studies suggest Tet as a promising candidate for DNP treatment, the precise mechanisms underlying its beneficial effects remain incompletely understood.

In the present study, it is hypothesized that Tet exerts its therapeutic effects through a dual mechanism: promoting a shift in microglial polarization from the pro-inflammatory M1 phenotype toward the anti-inflammatory M2 state and modulating neuronal autophagy. To test this hypothesis, a combined *in-vivo* and *in-vitro* approach was employed. First, a rat model of DNP was established to evaluate the therapeutic efficacy of Tet and to explore its underlying mechanisms. These mechanisms were further investigated *in-vitro* using high glucose-stimulated PC12 cells and lipopolysaccharide (LPS)-activated BV2 microglia.

MATERIALS AND METHODS

Experimental animals

Specific pathogen-free healthy male SD adult rats (6-7 weeks old, 220-250 g) were purchased from Beijing Vital River Laboratory Animal Technology Co., Ltd. (Beijing, China). The rats were given standard chow and clean water, maintained at 60% humidity, with a room temperature ranging from 21 to 26℃ and a 12-h light/dark cycle for one week prior to the experiment. The use of all animals was approved by the Experimental Ethics Committee of Institutional Animal Care and Use Committee of Zhejiang Chinese Medical University (Approval Number: 202402586[15]).

Rat model and treatment

Based on established protocols (J.W. Wang *et al*., 2022; Lee *et al*., 2024) with modifications, a DNP rat model was induced. Briefly, after a 16-hour fast, rats received a single intraperitoneal injection of streptozotocin (STZ; 65 mg/kg; Sigma-Aldrich, St. Louis, MO, USA) dissolved in sodium citrate buffer (pH 4.5). Control rats (n=12) were injected with an equal volume of citrate buffer. Diabetes was metabolically confirmed three days post-STZ injection using a fasting blood glucose (FBG) level ≥ 16.7 mmol/L measured from the tail vein. Behavioral phenotyping was then performed by monitoring the mechanical withdrawal threshold (MWT) and thermal withdrawal latency (TWL). Rats that displayed sustained reductions in both MWT and TWL below 85% of their pre-diabetes baseline at 14 days after STZ injection were defined as having DNP and included in subsequent experiments.

A total of thirty-six DNP rats were randomly allocated to three experimental groups using a computer-generated randomization sequence (n = 12 per group): the DNP model group, the low-dose Tet group (15 mg/kg) and the high-dose Tet group (30 mg/kg). Beginning 14 days after STZ injection, rats received daily oral gavage for 28 consecutive days with either saline (DNP model group) or the corresponding dose of Tet. The tetrandrine used (purity ≥ 98.0%) was obtained from Chengdu Alfa Biotechnology Co., Ltd. (Chengdu, China) and the selected doses were determined based on previous reports (L. Su *et al*., 2020; Z.L. Zhang *et al*., 2023) and optimized through preliminary experiments.

Body weight, FBG and behavioral tests were monitored on

a weekly basis throughout the entire study. Measurements commenced one week prior to STZ injection (establishing baseline values) and continued until the conclusion of the treatment phase. All behavioral assessments were conducted by experimenters blinded to group assignments. Testing was performed consistently at the same time of day in a dedicated, quiet behavioral room, following a standardized 30-minute acclimatization period for the animals. This longitudinal design enabled continuous tracking of neuropathic pain progression and precise evaluation of the time-dependent therapeutic effects of Tet, moving beyond a single endpoint to capture the dynamic response to treatment.

MWT assay

MWT in rats was measured using an automated Von Frey pain measurement instrument (Ugo Basile, Comerio, Italy). Approximately 30 minutes were given for the rats to acclimate to the test environment. The rats were placed on a metal mesh frame and their foot soles were stimulated mechanically with a metal wire, with a maximum force limit of 50 g to avoid injuries. Each rat was subjected to testing at least three times, with a minimum 5-minute interval before the second test and the average of these tests was calculated as the mechanical pain threshold for each rat.

TWL assay

The rats were allowed to acclimate in a clear plastic container for 30 minutes, after which their thermal pain threshold was assessed using a Hargreaves analgesiometer (Ugo Basile). An infrared light was pointed at the rat's hind paw and when the rat felt pain, it would retract its paw, at which time the reaction timer stopped and the time (seconds) was recorded. Each measurement was capped at 30 seconds to prevent injury. Testing was conducted on each rat at least three times, with a second test on the same rat performed after at least a 5-minute interval and the average of these tests was calculated as the thermal pain threshold for each rat.

Specimen collection

Upon completion of behavioral testing, rats were deeply anesthetized with an intraperitoneal injection of 3% pentobarbital sodium and transcardially perfused with ice-cold saline. The lumbar vertebral column was rapidly dissected to obtain the target tissues. For analyses of the spinal cord dorsal horn, the tissue was processed as follows: one portion was fixed in 4% paraformaldehyde for immunofluorescence, while the contralateral side was snap-frozen in liquid nitrogen for subsequent enzyme linked immunosorbent assay (ELISA) and reverse-transcription quantitative real-time polymerase chain reaction (RT-qPCR).

For Western blot analysis, the L4-L6 dorsal root ganglia (DRGs) were used. Under a surgical stereomicroscope, DRGs were visually identified adjacent to their corresponding intervertebral foramina, meticulously isolated from surrounding connective tissue and spinal nerves, promptly collected and then snap-frozen in liquid nitrogen. All frozen samples were stored at -80℃ until analysis.

Due to the limited amount of tissue obtainable from each rat, it was not feasible to conduct all analytical assays on the same animal. In strict adherence to the 3R principles (Replacement, Reduction, Refinement) endorsed by the ethics committee, the study was designed to minimize animal use while maximizing the information derived from each subject. Accordingly, for each major experimental analysis, tissues from a minimum of six randomly selected animals per group were used.

Immunofluorescence

The tissue sections underwent standard deparaffinization, rehydration and antigen retrieval via heat-mediated epitope unmasking. After blocking with normal serum, sections were incubated overnight at 4°C in a humidified chamber with the following primary antibodies: IBA1 (1:50, 10904-1-AP, Proteintech, Wuhan, China), iNOS (1:500, ab178945, Abcam, Cambridge, MA, USA) and CD206 (1:50, 18704-1-AP, Proteintech). Following thorough washing, sections were incubated with appropriate fluorophore-conjugated secondary antibodies for 2 hours at room temperature, protected from light. Nuclei were counterstained with DAPI (5 minutes) and slides were mounted with anti-fade medium. Images were captured using a Zeiss Axio Imager fluorescence microscope under consistent exposure settings. All images include a scale bar (50 μm) indicating magnification. For each tissue section, three non-overlapping fields of view were randomly selected for quantitative analysis. Microglial activation and phenotypic polarization were assessed using image J software (National Institutes of Health, Bethesda, MD, USA) by measuring either the mean fluorescence intensity of Iba1 (a specific microglial marker) or by counting double-positive cells ($iNOS^+Iba1^+$ for M1 phenotype; $CD206^+Iba1^+$ for M2 phenotype) within standardized regions of interest. To ensure objectivity, the entire process of tissue processing, image acquisition and data analysis was performed independently by two investigators under blinded conditions. The results from both observers were averaged for the final statistical analysis and inter-observer consistency was assessed to confirm reliability.

Cell culture and treatment

PC12 neuronal cell line and BV2 microglia cell line (ATCC, Manassas, VA, USA) were cultured in DMEM (GIBCO, Grand Island, NY, USA) containing 10% fetal bovine serum, 1% penicillin/streptomycin at 37°C in a 5% CO_2 humidified incubator.

PC12 and BV2 cells were first exposed to a range of Tet

concentrations for 24 hours in a CCK-8 assay to determine a non-cytotoxic working range. Based on these results and previous literature, appropriate concentrations were selected for subsequent experiments. In the mechanistic studies, PC12 cells were pre-treated with Tet for 1 hour, followed by exposure to high glucose (35 mmol/L) for 24 hours to mimic diabetic metabolic stress. Similarly, BV2 microglia were pre-treated with Tet for 1 hour and then stimulated with LPS (0.1 μg/mL; Sigma-Aldrich) for 24 hours to induce a pro-inflammatory state.

The concentrations of high glucose and LPS were selected according to well-established protocols in the literature, which reliably reproduce key pathological features: hyperglycemic stress in neuronal models (Yuan *et al*. 2023) and neuroinflammatory activation in microglial cells (Choi *et al*. 2024; Lin *et al*. 2025). These conditions were further validated in the preliminary experiments (including CCK-8 and pilot cytokine measurements) to ensure they elicited a robust and reproducible cellular response without without causing excessive cell death.

CCK-8

Cells in 96-well plates were planted at 2×10^4 per well and incubated overnight prior to treatment. Subsequently, a mixture of 10 μL CCK-8 solution (Solarbio, Beijing, China) and 100 μL of DMEM was prepared and kept at 37°C for 4 hour. Absorbance was recorded at 450 nm using an automated microplate reader.

ELISA

Collected tissues were weighed and placed in ice-cold radioimmunoprecipitation assay (RIPA) lysis buffer supplemented with protease and phosphatase inhibitors (Thermo Fisher Scientific, Waltham, MA, USA). Homogenization was performed on ice using a motorized tissue grinder and the resulting lysates were centrifuged at 12,000 × g for 15 minutes at 4 °C. The supernatants were collected, aliquoted and stored at -80 °C before analysis. For cells, culture supernatants were collected and centrifuged to remove debris before analysis. Levels of TNF-α, IL-1β and IL-6 were measured using commercially available ELISA kits (R&D Systems, MN, USA) according to the manufacturer's protocols. All samples were run in duplicate. Cytokine concentrations in tissue homogenates were normalized to total protein content and expressed as pg/mg protein. Concentrations in cell supernatants were expressed as pg/mL.

Western blot

Total protein was extracted from tissues and cultured cells using RIPA buffer (Beyotime, Shanghai, China). Protein concentration was determined with a BCA Protein Assay Kit (Beyotime). Equal amounts of protein were separated by 10% sodium dodecyl sulfate-polyacrylamide gel electrophoresis (SDS-PAGE) and then transferred onto polyvinylidene fluoride (PVDF) membranes. After blocking with 5% non-fat milk for 2 h at room temperature, the membranes were incubated overnight at 4 °C with the following primary antibodies: anti-Beclin-1 (1:1000, #3495, Cell Signaling Technology, Danvers, MA, USA,), anti-LC3B (1:1000, ab192890, Abcam), anti-p62 (1:1000, ab109012, Abcam), anti-PINK1 (1:1000, A7131, Abclonal, Wuhan, China), anti-parkin (1:1000, Abclonal, A0968) and anti-β-actin (1:5000, 20536-1-AP, Proteintech). Following washes, membranes were incubated with horseradish peroxidase (HRP)-conjugated IgG secondary antibody (1:5000, Abcam) for 1 hours at 37 °C. Protein bands were visualized using enhanced chemiluminescence (ECL) substrate (Pierce, Rockford, IL, USA) and imaged with a gel documentation system. Band intensities were quantified with ImageJ software (National Institutes of Health). Target protein expression was normalized to β-actin. For the analysis of LC3, both the LC3-II/LC3-I ratio and the level of LC3-II normalized separately to β-actin were calculated and reported.

RT-qPCR

Total RNA was extracted from tissues and cells using TRIzol reagent (Invitrogen, Carlsbad, CA, USA). RNA concentration was quantified using a Beckman UV spectrophotometer and its integrity was assessed via agarose gel electrophoresis. Complementary DNA (cDNA) was synthesized from 1 μg of total RNA using a reverse transcription kit (Thermo Fisher Scientific, Waltham, MA, USA). Quantitative real-time PCR was performed with the Ultra SYBR Mixture (Takara Bio, Otsu, Japan) on an ABI 7500 PCR system (Applied Biosystems, CA, USA). All primer sequences were synthesized by Sangon Biotech (Shanghai, China) and are listed in table 1. The expression of each target gene was normalized to the endogenous reference gene β-actin and calculated using the $2^{-\Delta\Delta Ct}$ method.

Blinding and quality control

To ensure objectivity and minimize bias, all behavioral tests, histological procedures and subsequent evaluations were performed by experimenters who were blinded to the experimental group assignments. Furthermore, all quantitative data were independently verified by a second researcher to ensure accuracy and reproducibility.

Statistical analysis

Sample sizes were determined through a priori power analysis conducted with G*Power software (version 3.1, Düsseldorf, Germany), using an α level of 0.05, a power of 0.80 and effect sizes estimated from previous comparable studies or pilot experiments. All data are presented as mean ± standard deviation (SD). Homogeneity of variance and normality of distribution were evaluated using Levene's test and the Shapiro-Wilk test, respectively. For comparisons between two groups, an unpaired two-tailed Student's t-test was used for data meeting parametric assumptions; otherwise, the Mann-Whitney U test was

applied. For comparisons among multiple groups under a single independent variable, one-way ANOVA was performed, followed by Tukey's post-hoc test. For data involving two independent variables (e.g., treatment and time), two-way ANOVA with repeated measures (where applicable) was used, also followed by Tukey's test. If data violated parametric assumptions, the non-parametric Kruskal–Wallis test with Dunn's post-hoc correction was employed. All statistical analyses were performed using GraphPad Prism (version 10.0; GraphPad Software, San Diego, CA, USA). A P-value < 0.05 was considered statistically significant.

RESULTS

Tet attenuates neuropathic pain in DNP rats

Rats received a single high-dose intraperitoneal injection of STZ to induce DNP. As shown in figs 1A and 1B, STZ administration resulted in a significant increase in FBG and a decrease in body weight compared to controls. Concomitantly, both the MWT and TWL were significantly reduced from baseline, confirming the development of robust pain hypersensitivity (Figs. 1C and 1D; Table S1).

To evaluate the therapeutic potential of Tet, STZ-induced rats were treated daily with a low or high dose of Tet for four weeks, beginning two weeks after STZ injection. Tet treatment was associated with a modest, non-significant reduction in FBG and a trend toward weight recovery in the later stages (weeks 5-6) (Figs. 1A and 1B). In contrast, pain-related behaviors showed marked and dose-dependent improvement. The change from baseline in both MWT and TWL was significantly reversed in Tet-treated groups compared to the DNP model group, with the most substantial recovery observed between the fourth and sixth weeks post-STZ (Figs. 1C and 1D). The high-dose Tet regimen consistently produced stronger anti-hyperalgesic effects than the low-dose treatment.

Tet reverses microglial polarization and neuroinflammation in DNP rats

To evaluate the effect of Tet on microglial polarization in DNP, the expression of phenotype-specific markers was examined. RT-qPCR analysis showed that Tet treatment significantly downregulated M1-associated genes (iNOS, CD16, CD32) and upregulated M2-associated genes (Arg1, CD206, IL-10) in the spinal cord dorsal horn of DNP rats (Figs. 2A and 2B), indicating a shift from a pro-inflammatory M1 toward an anti-inflammatory M2 phenotype. Immunofluorescence results were consistent with the transcriptional data. Tet treatment effectively reduced the number of M1 phenotype cells ($iNOS^+Iba1^+$) while increasing the number of M2 phenotype cells ($CD206^+Iba1^+$) (Fig. 2C and 2D). Together, these findings demonstrate that Tet reprograms microglial polarization toward the anti-inflammatory M2 state in DNP.

Consistently, Tet treatment effectively suppressed this neuroinflammatory response, as evidenced by a significant reduction in both the fluorescence intensity of the total microglial marker Iba-1 (Fig. 2D) and the levels of pro-inflammatory cytokines (TNF-α, IL-1β and IL-6) (Fig. 2E) in the spinal cord dorsal horn, with the high-dose group showing a more pronounced effect.

Tet regulates neuronal autophagy-related protein expression in DNP rats

Next, the effect of Tet on autophagic activity in the spinal cord of DNP rats was examined. Western blot analysis showed that, compared with the control group, DNP rats exhibited a slight increase in both the LC3-II/LC3-I ratio and LC3-II protein level, a decrease in the autophagic substrate p62, while Beclin-1 levels showed no significant change (Fig. 3A). After Tet treatment, the expression of Beclin-1, the LC3-II/LC3-I ratio and the level of LC3-II were all significantly upregulated and p62 accumulation was further reduced (Fig. 3A). These changes suggest a potential activation of the autophagic process. Furthermore, the expression of PINK1 and parkin was significantly downregulated in DNP rats, while Tet administration effectively restored the levels of both proteins (Fig. 3B), indicating an improvement in the mitophagy signaling pathway.

In summary, Tet may promote a functional autophagic response in the DNP state, as evidenced by the upregulation of key autophagy-initiation and mitophagy-related proteins, along with a reduction in autophagic substrate accumulation.

Tet shifts BV2 microglia from M1 to M2 phenotype

CCK-8 experiments to observe the toxic effects of Tet on BV2 microglia revealed that the proliferative activity of BV2 cells was significantly inhibited when the concentration of Tet exceeded 5 μM (Fig. 4A), and therefore, subsequent experiments were performed using Tet at concentrations less than 5 μM.

To investigate whether Tet exerts a consistent effect on microglial polarization *in-vitro*, BV2 cells were stimulated with LPS to simulate the inflammatory microenvironment of DNP. Tet treatment significantly downregulated the expression of M1-related genes (iNOS, CD16, CD32) and upregulated M2-related genes (Arg1, CD206, IL-10) in LPS-activated BV2 cells (Figs. 4B and 4C), indicating that Tet promotes a phenotypic shift from the M1 to the M2 state in microglia.

Consistently, ELISA analysis of BV2 cell culture supernatants showed that Tet markedly suppressed the LPS-induced elevation of pro-inflammatory cytokines, including TNF-α, IL-1β and IL-6 (Fig. 4D). These *in-vitro* results align with the *in-vivo* observations, further supporting the role of Tet in modulating microglial polarization toward an anti-inflammatory phenotype.

Table 1: Primers.

Species	Genes	Forward primer (5′–3′)	Reverse primer (5′–3′)
Mouse	CD16	TTTGGACACCCAGATGTTTCAG	GTCTTCCTTGAGCACCTGGATC
	CD32	AATCCTGCCGTTCCTACTGATC	GTGTCACCGTGTCTTCCTTGAG
	iNOS	GCGCAAAACATTTCCTGGGAG	CTGGAACATTCTGTGCTGTCCC
	CD206	CAAGGAAGGTTGGCATTTGT	CCTTTCAGTCCTTTGCAAGC
	Arg1	AAGCCTGGTCTGCTGGAAAAA	CTGGTTGTCAGGGGAGTGTT
	IL-10	CGGGAAGACAATAACTGCACCC	CGGTTAGCAGTATGTTGTCCAGC
	β-actin	CCTAGACTTCGAGCAAGAGA	GGAAGGAAGGCTGGAAGA
Rats	CD16	ACTGTGGTTGGCTTTTGGGAT	GAGTGATTTCTGACTGGCTGCTG
	CD32	CCAGAAAGGCCAGGATCTAGTG	GGGAACCAATCTCGTAGTGTCTGT
	iNOS	GGTGAGGGGACTGGACTTTT	TTCTCCGTGGGGCTTGTAGT
	CD206	TCAACTCTTGGACTCACGGC	ATGATCTGCGACTCCGACAC
	Arg1	AGTGTGGTGCTGGGTGGAG	GCGGAGTGTTGATGTCAGTGTG
	IL-10	TGAACCACCCGGCATCTACT	CCAAGGAGTTGCTCCCGTTA
	β-actin	TACTGCCCTGGCTCCTAGCA	TGGACAGTGAGGCCAGGATAG

Note: iNOS, inducible nitric oxide synthase; Arg1, arginase1; IL-10, interleukin-10.

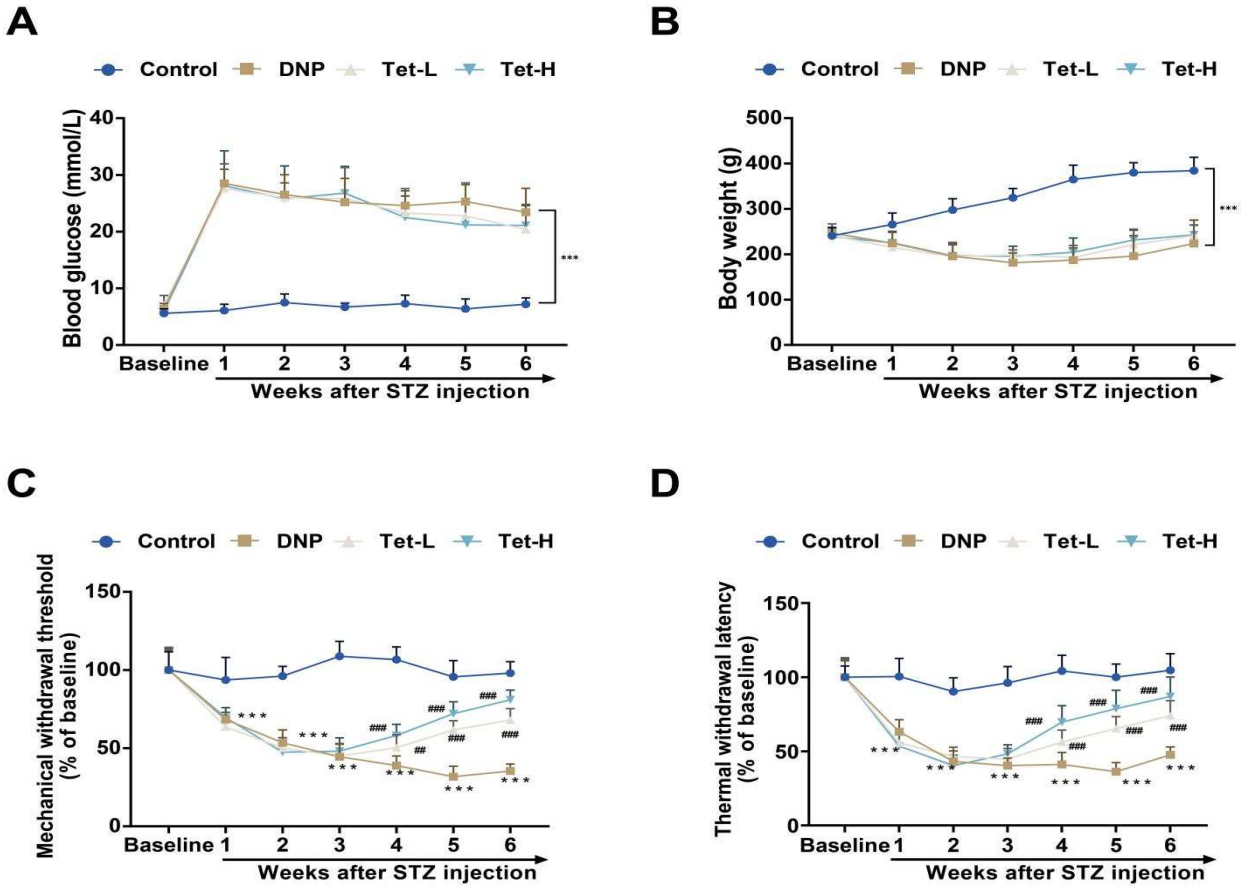

Fig. 1: Tet attenuates neuropathic pain in DNP rats.
Rats received a single intraperitoneal injection of STZ (65 mg/kg), with the day of injection designated as day 0. Starting from day 14 post-STZ, animals were treated daily by oral gavage with either normal saline or Tet (15 or 30 mg/kg) for 28 consecutive days. Body weight, FBG, and behavioral responses were assessed at baseline (pre-STZ) and weekly thereafter for 6 weeks. (A) FBG (mmol/L) over time; (B) Body weight (g) over time; (C) MWT over time; (D) TWL over time. Data are presented as mean ± SD. Statistical analysis was performed using two-way ANOVA with repeated measures followed by Tukey's multiple comparisons test (*$P < 0.05$, **$P < 0.01$, ***$P < 0.001$ vs. Control group; $^{\#}P < 0.05$, $^{\#\#}P < 0.01$, $^{\#\#\#}P < 0.001$ vs. DNP group; n = 12 rats per group).

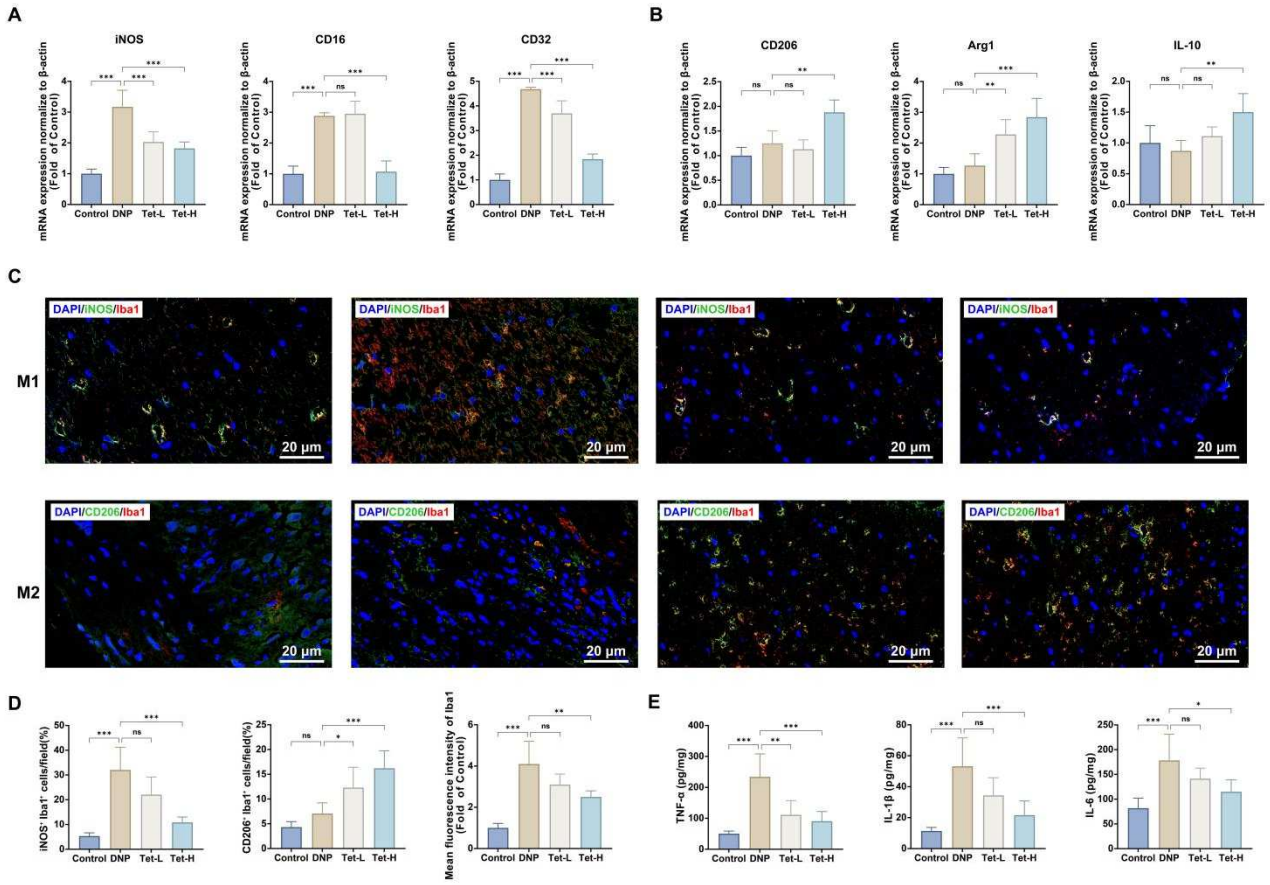

Fig. 2: Tet reverses microglial polarization and neuroinflammation in DNP rats
(A) mRNA expression of M1-related genes (iNOS, CD16, CD32) in the spinal cord dorsal horn measured by RT-qPCR; (B) mRNA expression of M2-related genes (CD206, Arg1, IL-10) in the spinal cord dorsal horn measured by RT-qPCR; (C) Representative immunofluorescence images of the spinal cord dorsal horn in rats. Sections were stained for nuclei (DAPI, blue), total microglia (Iba1, red), M1-phenotype microglia (iNOS, green), M2-phenotype microglia (CD206, green); (D) Quantitative analysis of microglial response: mean fluorescence intensity of Iba1, number of $iNOS^{+}Iba1^{+}$ cells (M1), and number of $CD206^{+}Iba1^{+}$ cells (M2); (E) Levels of pro-inflammatory cytokines (TNF-α, IL-1β, and IL-6) measured by ELISA in spinal cord dorsal horn tissue homogenates. Data are presented as mean ± SD (n = 6 rats/group). Statistical significance was determined by one-way ANOVA followed by Tukey's post hoc test (*$P < 0.05$, **$P < 0.01$, ***$P < 0.001$; ns, not significant).

In-vitro assessment of tetrandrine on neuronal autophagy

The potential cytotoxicity of Tet was first assessed in PC12 cells using the CCK-8 assay. Cell viability was significantly reduced at concentrations above 5 μM (Fig. 5A); therefore, all subsequent experiments used Tet at concentrations 5 μM to ensure cellular health.

Under high-glucose conditions, Tet treatment in PC12 cells significantly increased the expression of Beclin-1, elevated the LC3-II/LC3-I ratio and LC3-II protein levels and effectively reduced p62 accumulation (Fig. 5B). These changes in static autophagy markers suggest that Tet enhances autophagic activity. Furthermore, high glucose markedly suppressed the expression of the mitophagy-initiating proteins PINK1 and parkin, while Tet treatment counteracted this suppression and restored their protein levels (Fig. 5C). Collectively, these *in-vitro* results demonstrate that Tet positively modulates the expression of key markers associated with both general autophagy and mitophagy in neurons under glucotoxic stress.

DISCUSSION

In the present study, a single intraperitoneal injection of STZ successfully induced DNP in rats. Tet treatment significantly alleviated neuropathic pain and attenuated spinal neuroinflammation in this model, with effects being more pronounced at higher doses. These protective actions align with and extend previous reports on the beneficial effects of Tet in diabetes and neuropathic pain conditions (L. Su *et al*., 2020; Z.L. Zhang *et al*., 2023).

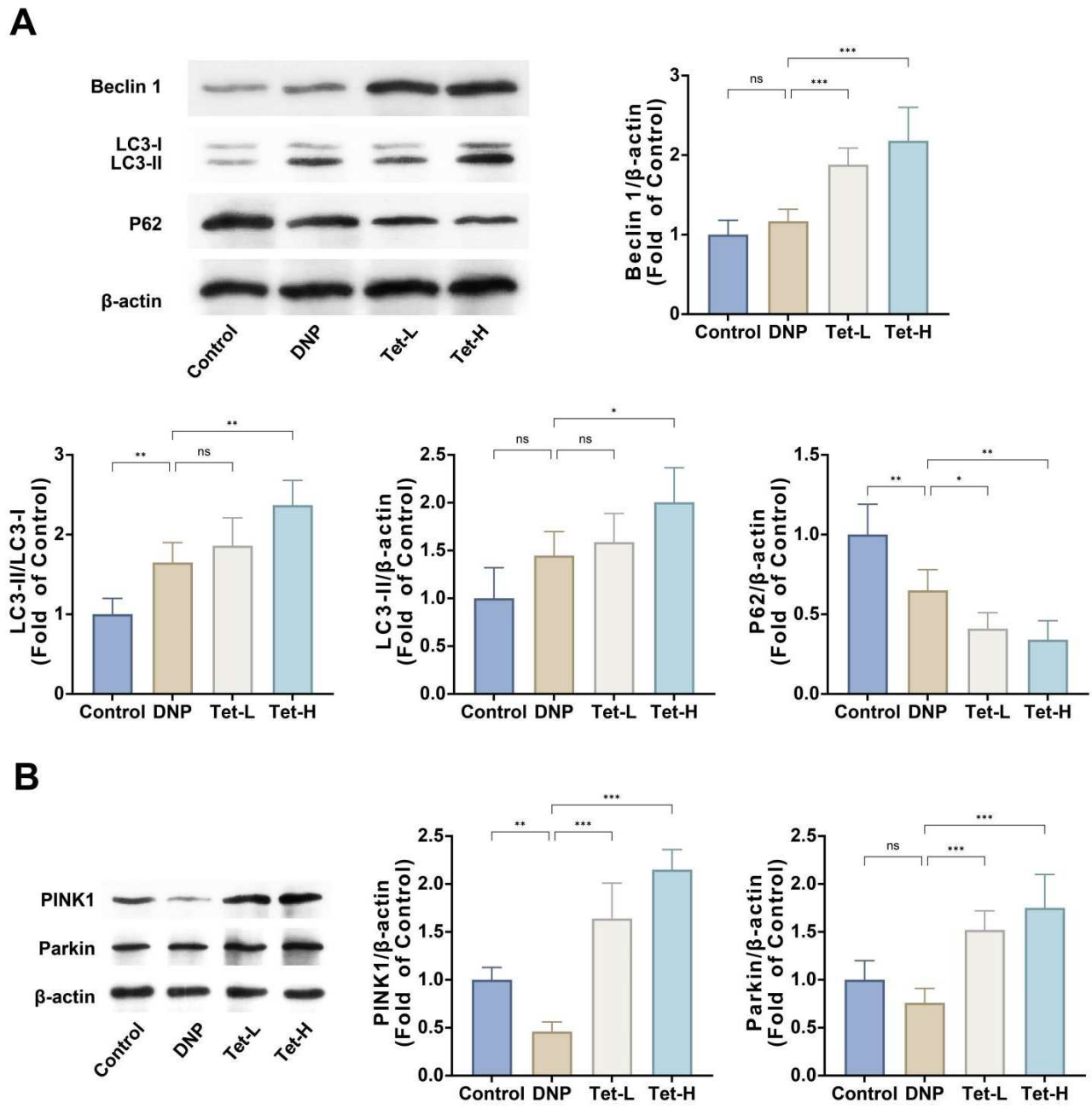

Fig. 3: Tetrandrine regulates neuronal autophagy-related protein expression in DNP Rats.
(A) Representative Western blot images and quantitative analysis of Beclin-1, the LC3-II/LC3-I ratio, LC3-II level, and p62 in DRG tissues; (B) Representative Western blot images and quantitative analysis of PINK1 and parkin in DRG tissues. Data are presented as mean ± SD (n = 6 rats/group). Statistical significance was determined by one-way ANOVA followed by Tukey's post hoc test (*$P < 0.05$, **$P < 0.01$, ***$P < 0.001$; ns, not significant).

Neuroinflammation, marked by immune cell infiltration and microglial activation following nerve injury, is a central pathological driver of DNP. Upon activation, microglia release pro-inflammatory cytokines and mediators, which further reinforce their own polarization through autocrine signaling. This self-amplifying response perpetuates neuroinflammation, exacerbates pain transmission and contributes to chronic pain persistence (An *et al*., 2025). Tet has demonstrated anti-neuroinflammatory properties. For example, intrathecal administration of Tet has been shown to alleviate traumatic spinal cord injury by modulating the activation of neurotoxic microglia and astrocytes (Xu *et al*., 2025).

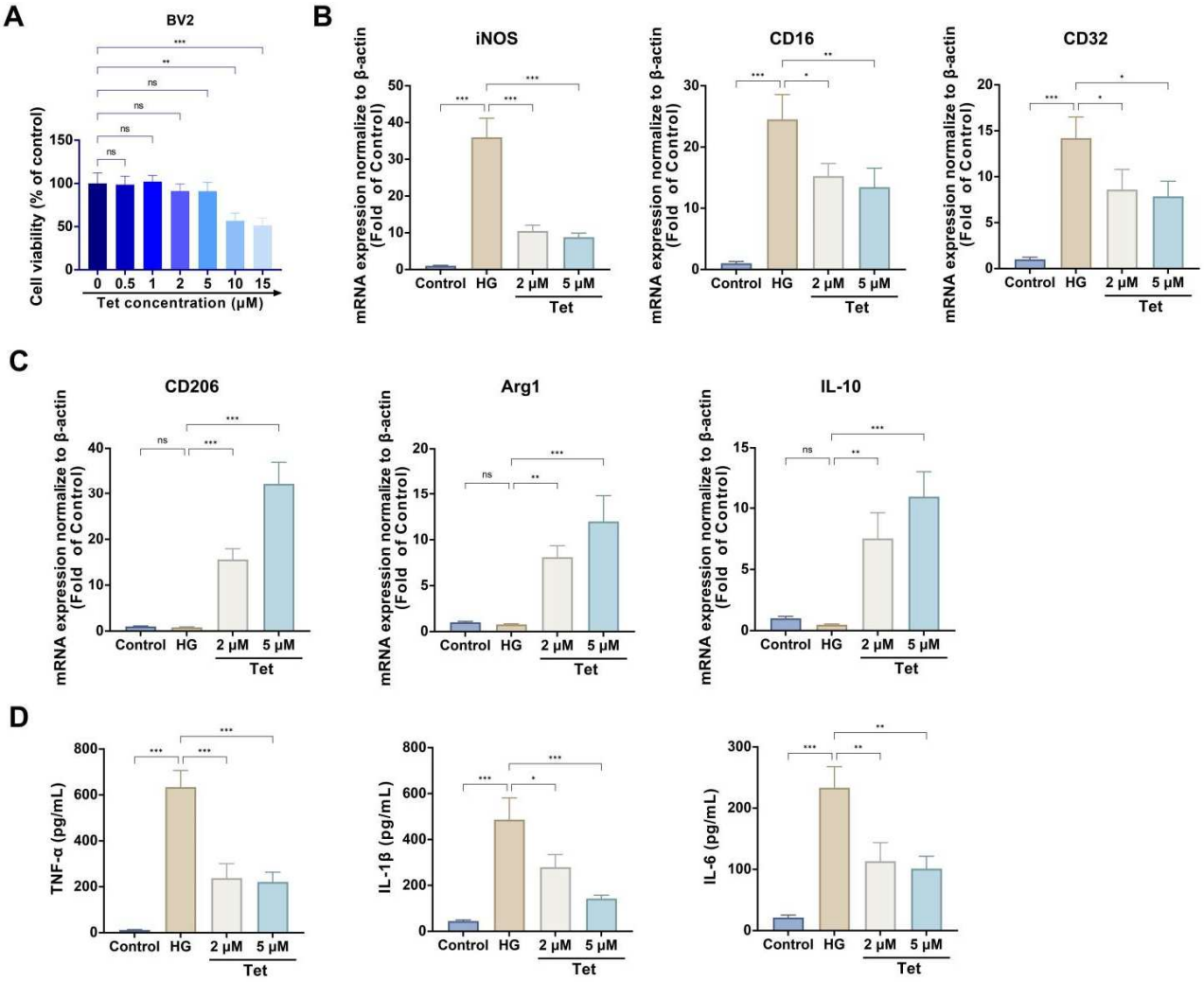

Fig. 4: Tet shifts BV2 microglia from M1 to M2 phenotype.
(A) Cell viability assessed by CCK-8 assay in BV2 microglia treated with Tet; (B) RT-qPCR analysis of M1-related genes (iNOS, CD16, CD32) in LPS-stimulated BV2 cells with or without Tet treatment; (C) RT-qPCR analysis of M2-related genes (CD206, Arg1, IL-10) under the same conditions; (D) Levels of pro-inflammatory cytokines (TNF-α, IL-1β, IL-6) in the supernatant of cells under the same conditions measured by ELISA. Data are presented as mean ± SD from three independent experiments. Statistical significance was determined by one-way ANOVA followed by Tukey's post hoc test (*$P < 0.05$, **$P < 0.01$, ***$P < 0.001$; ns, not significant).

Consistent with this, it was found that spinal neuroinflammation was suppressed and the M1 polarization of microglia was attenuated in DNP rats following Tet treatment. *In-vitro* experiments further confirmed that Tet promotes a phenotypic shift from pro-inflammatory M1 toward anti-inflammatory M2 in LPS-stimulated BV2 microglia, aligning with a previous report on its immunomodulatory effects in glial cells (Ren *et al*., 2021). These findings collectively underscore that modulating microglial phenotypic transition is a crucial mechanism underlying the therapeutic efficacy of Tet in DNP. Growing evidence underscores the complex, context-dependent role of autophagy in neuropathic diseases. Appropriately activated autophagy within the nervous system can exert analgesic effects in conditions such as DPN, with the functional outcome heavily reliant on the integrity of the complete autophagic flux (Gao *et al*., 2023). Tet has been documented to modulate autophagy across various disease models, though its effects are context-specific, functioning as either an inducer or an inhibitor (Bhagya and Chandrashekar, 2022; H. Liu *et al*. 2022; Tong *et al*. 2022). Therefore, clarifying its precise role in neuronal autophagy warranted further investigation. In our study, compared to control rats, DNP rats exhibited a modest increase in the LC3-II/LC3-I ratio and LC3-II level alongside a decrease in p62, a pattern that might initially suggest enhanced autophagic flux (He *et al*., 2022). However, no significant change was observed in Beclin-1, a key initiator of autophagosome formation.

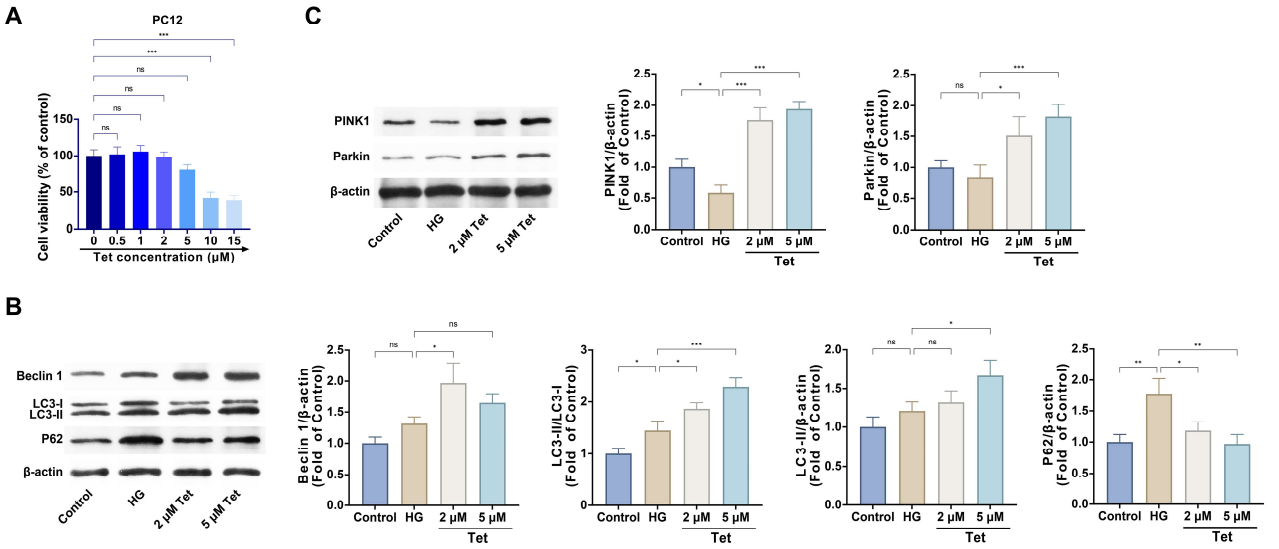

Fig. 5 *In-vitro* assessment of tetrandrine on neuronal autophagy.
(A) Cell viability of PC12 cells treated with Tet assessed by CCK-8 assay; (B) Western blot analysis and quantification of Beclin-1, the LC3-II/LC3-I ratio, LC3-II level and p62 in high glucose-stimulated PC12 cells with or without Tet treatment; (C) Western blot analysis and quantification of PINK1 and parkin under the same conditions. Data are presented as mean ± SD from three independent experiments. Statistical significance was determined by one-way ANOVA followed by Tukey's post hoc test (*$P < 0.05$, **$P < 0.01$, ***$P < 0.001$; ns, not significant).

More importantly, a concurrent and marked reduction in the key mitophagy-initiating proteins PINK1 and parkin was detected. PINK1 plays a crucial role in initiating mitophagy by recruiting its downstream effector parkin upon mitochondrial damage; together, they regulate the mitophagy process, which is essential for maintaining mitochondrial quality and cellular function (C.J. Su *et al*., 2020). A recent study has shown that hyperglycemia disrupts the PINK1/parkin mitochondrial autophagy pathway, resulting in reduced mitochondrial stability, cell death and toxic effects on ND7/23 cells (Bian *et al*., 2025). Therefore, activating or restoring mitophagy via the PINK1 pathway might offer a promising therapeutic strategy for DNP. These findings provide crucial context, indicating a specific deficit in the upstream recognition and targeting of damaged mitochondria for clearance (i.e., mitophagy) under disease conditions. Such an impairment at the initiation stage could lead to an incomplete or dysfunctional overall autophagic response, which aligns with the broader concept of "autophagy impairment" in the diseased state. Tet treatment in DNP rats elevated Beclin-1 levels, further increased the LC3-II/LC3-I ratio and LC3-II and decreased p62 accumulation. More importantly, Tet administration effectively restored suppressed expression of PINK1 and parkin in both DNP rats and high-glucose-stressed PC12 cells. This suggests that Tet may reactivate mitophagic signaling, a process critical for maintaining neuronal health by mitigating oxidative stress and apoptosis (Yao *et al*., 2024). This conclusion is further supported by prior studies indicating that Tet induces mitophagy via the PINK1/parkin pathway (X.H. Wang *et al*., 2021; Chu *et al*., 2024).

Several limitations of the present study should be acknowledged. First, the interpretation of autophagy is based on static protein markers. Although the observed changes are consistent with modulated autophagic and mitophagic activity, a definitive distinction cannot be made between enhanced flux and a potential blockade at the degradation stage. Future studies employing autophagic flux assays and functional mitochondrial assessments are essential to confirm the functional outcomes of Tet intervention. Second, while the *in-vivo* dosing of Tet was based on established protocols from prior studies and refined through preliminary tests, detailed pharmacokinetic, toxicity, or tissue distribution data were not provided. This information would strengthen the translational relevance of our findings and is an important focus for subsequent preclinical development. Third, the *in-vitro* concentrations of Tet were selected based on literature precedents and validated in pilot experiments for their ability to induce relevant phenotypes without excessive cytotoxicity. Although a full multi-point dose-response analysis for all parameters was beyond the primary mechanistic scope, a more comprehensive pharmacological characterization in future work would help optimize the therapeutic window. Finally, the cellular models used (PC12 and BV2 cells) offer valuable but simplified systems. PC12 cells are not primary sensory neurons and BV2 microglia differ from primary microglia in key aspects. While these models are suitable for initial mechanistic exploration, the findings need to be confirmed in more physiologically relevant systems, such as primary sensory neurons and microglia, as a necessary next step.

CONCLUSION

Tet treatment effectively alleviates DNP and associated neuroinflammation in rats, likely through modulating microglial phenotypic transition and neuronal autophagy. These findings provide novel insights and experimental support for the potential therapeutic use of Tet in DNP management.

Acknowledgments
None.

Authors' contribution
Q.Z. Liu: Designed the research study. Provided help and advice on the experiments; Q.Z. Liu and H. Zhang: wrote the manuscript; H. Zhang: Performed the research and analyzed the data. Both authors contributed to editorial changes in the manuscript. All authors read and approved the final manuscript.

Funding
Zhejiang Medical Science and Technology Development Program (2023KY963).

Data availability
The datasets generated and/or analyzed during the current study are available from the corresponding author on reasonable request.

Ethical approval
The present study was approved by the Institutional Animal Care and Use Committee of Zhejiang Chinese Medical University. All procedures complied with the National Institutes of Health Guide for the Use of Laboratory Animals (Approval Number: 202402586[15]). This study was performed in adherence with the ARRIVE guidelines. See supplementary file for the ARRIVE checklist.

Conflict of interest
The authors declare no conflict of interest.

Supplementary data
https://www.pjps.pk/uploads/2026/06/SUP1782455983.pdf

REFERENCES

Antar SA, Ashour NA, Sharaky M, Khattab M, Ashour NA, Zaid RT, Roh EJ, Elkamhawy A and Al-Karmalawy AA (2023). Diabetes mellitus: Classification, mediators and complications; A gate to identify potential targets for the development of new effective treatments. *Biomed. Pharmacother.*, **168**: 115734.

An Y, Cao S, Shi L, Zhang Y, Wang X, Yuan S, Shi Y, Wang B, Liu J and Han CJ (2025). Pharmacological modulation of Sigma-1 receptor ameliorates pathological neuroinflammation in rats with diabetic neuropathic pain via the AKT/GSK-3β/NF-κB pathway. *Brain. Res. Bull.,* **221**: 111226.

Bhagya N and Chandrashekar KR (2022). Autophagy and cancer: Can tetrandrine be a potent anticancer drug in the near future? *Biomed. Pharmacother.,* **148**: 112727.

Bhandari R, Sharma A and Kuhad A (2021). Novel nanotechnological approaches for targeting dorsal root ganglion (DRG) in mitigating diabetic neuropathic pain (DNP). *Front. Endocrinol (Lausanne).,* **12**: 790747.

Bian Y, Yang Y, Chen J, Liu J, Tao Y, Liu Z and Huang L (2025). Defective PINK1-dependent mitophagy is involved in high glucose-induced neurotoxicity. *Neuroscience.,* **573**: 286-299.

Braffett BH, El Ghormli L, Albers JW, Feldman EL, Herman WH, Gubitosi-Klug RA, Martin CL, Orchard TJ, White NH, Lachin JM, Perkins BA and Pop-Busui R (2024). Neuropathic pain with and without diabetic peripheral neuropathy in type 1 diabetes. *Diabetes. Care.,* **47**(9): 1559-1567.

Breitinger U and Breitinger HG (2023). Excitatory and inhibitory neuronal signaling in inflammatory and diabetic neuropathic pain. *Mol. Med.,* **29**(1): 53.

Chen Y, Deng H and Zhang N (2025). Autophagy-targeting modulation to promote peripheral nerve regeneration. *Neural. Regen. Res.*, **20**(7): 1864-82.

Choi JW, Choi SY, Yoo G, Park HY, Choi IW and Hur J (2024). *Melissa officinalis* regulates lipopolysaccharide-induced BV2 microglial activation via MAPK and Nrf2 signaling. *J. Microbiol. Biotechnol.*, **34**(12): 2474-83.

Chong ZZ and Souayah N (2025). Neuroinflammation in diabetic peripheral neuropathy and therapeutic implications. *Rev. Neurosci.,* **36**(7): 749-762.

Chu L, Zhuo J, Huang H, Chen W, Zhong W, Zhang J, Meng X, Zou F, Cai S, Zou M and Dong H (2024). Tetrandrine alleviates pulmonary fibrosis by inhibiting alveolar epithelial cell senescence through PINK1/Parkin-mediated mitophagy. *Eur. J. Pharmacol.,* **969**: 176459.

Ding Y (2025). Histone deacetylases: The critical enzymes for microglial activation involved in neuropathic pain. *Front. Pharmacol.,* **16**: 1515787.

Duran AM, Zamora F and De León M (2024). Dietary docosahexaenoic acid-rich supplementation decreases neurotoxic lipid mediators in participants with type 2 diabetes and neuropathic pain. *Nutrients.,* **16**(23): 4025.

Fan K, Liao Q, Yuan P, Xu R and Liu Z (2024). Defective autophagy contributes to bupivacaine-induced aggravation of painful diabetic neuropathy in db/db mice. *Neuropharmacology.,* **245**: 109814.

Gao N, Ma B, Jia H, Hao C, Jin T and Liu X (2023). Translocator protein alleviates allodynia and improves Schwann cell function against diabetic peripheral neuropathy via activation of the Nrf2-dependent antioxidant system and promoting autophagy. *Diabet. Med.,* **40**(6): e15090.

Gazzeri R, Mosca J, Occhigrossi F, Galarza M, Schiaffini R, Varrassi G, Mercieri M and Leoni MLG (2025).

Spinal cord stimulation in painful diabetic neuropathy: Advances, outcomes and future directions. *Biomedicines.*, **13**(12): 3063.

Gong L, Liu H, Xu B, Yu T, Wang Y, Niu SL, Zeng R and Ouyang Q (2024). Insights on exploring the therapeutic potential and structural modification of Tetrandrine. *Future. Med. Chem.,* **16**(24): 2687-2700.

He J, Qin Z, Chen X, He W, Li D, Zhang L, Le Y, Xiong Q, Zhang B and Wang H (2022). HIF-1α ameliorates diabetic neuropathic pain via parkin-mediated mitophagy in a mouse model. *Biomed. Res. Int.,* **2022**: 5274375.

Jang HN and Oh TJ (2023). Pharmacological and nonpharmacological treatments for painful diabetic peripheral neuropathy. *Diabetes. Metab. J.,* **47**(6): 743-756.

Karpova A, Hiesinger PR, Kuijpers M, Albrecht A, Kirstein J andres-Alonso M, Biermeier A, Eickholt BJ, Mikhaylova M, Maglione M, Montenegro-Venegas C, Sigrist SJ, Gundelfinger ED, Haucke V and Kreutz MR (2025). Neuronal autophagy in the control of synapse function. *Neuron.*, **113**(7): 974-90.

Klionsky DJ, Petroni G, Amaravadi RK, Baehrecke EH, Ballabio A, Boya P, Bravo-San Pedro JM, Cadwell K, Cecconi F, Choi AMK, Choi ME, Chu CT, Codogno P, Colombo MI, Cuervo AM, Deretic V, Dikic I, Elazar Z, Eskelinen EL, Fimia GM, Gewirtz DA, Green DR, Hansen M, Jäättelä M, Johansen T, Juhász G, Karantza V, Kraft C, Kroemer G, Ktistakis NT, Kumar S, Lopez-Otin C, Macleod KF, Madeo F, Martinez J, Meléndez A, Mizushima N, Münz C, Penninger JM, Perera RM, Piacentini M, Reggiori F, Rubinsztein DC, Ryan KM, Sadoshima J, Santambrogio L, Scorrano L, Simon HU, Simon AK, Simonsen A, Stolz A, Tavernarakis N, Tooze SA, Yoshimori T, Yuan J, Yue Z, Zhong Q, Galluzzi L and Pietrocola F (2021). Autophagy in major human diseases. *Embo. j.,* **40**(19): e108863.

Kuthati Y, Rao VN, Huang WH, Busa P and Wong CS (2023). Teneligliptin co-infusion alleviates morphine tolerance by inhibition of spinal microglial cell activation in streptozotocin-induced diabetic Rats. *Antioxidants. (Basel).,* **12**(7): 1478.

Lee SO, Kuthati Y, Huang WH and Wong CS (2024). Semaglutide ameliorates diabetic neuropathic pain by inhibiting neuroinflammation in the spinal cord. *Cells.,* **13**(22): 1857.

Li X, Liu Y, Jing Z, Fan B, Pan W, Mao S and Han Y (2023). Effects of acupuncture therapy in diabetic neuropathic pain: A systematic review and meta-analysis. *Complement. Ther. Med.,* **78**: 102992.

Lin X, Xia Y, Yang X, Niu P, Wang H, Liu W, Huang J and Lin F (2025). TRIM14 Inhibition Suppresses Microglial Polarization and pyroptosis through the NF-κB/NLRP3 pathway to enhance spinal cord injury repair. *Mediators. Inflamm.*, **2025**: 5053685.

Liu H, He S, Wang J, Li C, Liao Y, Zou Q and Chen R (2022). Tetrandrine ameliorates traumatic brain injury by regulating autophagy to reduce ferroptosis. *Neurochem. Res.*, **47**(6): 1574-87.

Liu S, Yao S, Yang H, Liu S and Wang Y (2023). Autophagy: Regulator of cell death. *Cell. Death. Dis.,* **14**(10): 648.

Puglisi-Allegra S, Lazzeri G, Busceti CL, Giorgi FS, Biagioni F and Fornai F (2023). Lithium engages autophagy for neuroprotection and neuroplasticity: Translational evidence for therapy. *Neurosci. Biobehav. Rev.*, **148**: 105148.

Ren D, Fu Y, Wang L, Liu J, Zhong X, Yuan J, Jiang C, Wang H and Li Z (2021). Tetrandrine ameliorated Alzheimer's disease through suppressing microglial inflammatory activation and neurotoxicity in the 5XFAD mouse. *Phytomedicine.,* **90**: 153627.

Si W, Li X, Jing B, Chang S, Zheng Y, Chen Z, Zhao G and Zhang D (2024). Stigmasterol regulates microglial M1/M2 polarization via the TLR4/NF-κB pathway to alleviate neuropathic pain. *Phytother. Res.,* **38**(1): 265-279.

Su CJ, Shen Z, Cui RX, Huang Y, Xu DL, Zhao FL, Pan J, Shi AM, Liu T and Yu YL (2020). Thioredoxin-interacting protein (TXNIP) regulates parkin/PINK1-mediated mitophagy in dopaminergic neurons under high-glucose conditions: Implications for molecular links between Parkinson's disease and diabetes. *Neurosci. Bull.,* **36**(4): 346-358.

Su L, Cao P and Wang H (2020). Tetrandrine mediates renal function and redox homeostasis in a streptozotocin-induced diabetic nephropathy rat model through Nrf2/HO-1 reactivation. *Ann. Transl. Med.,* **8**(16): 990.

Tong BC, Huang AS, Wu AJ, Iyaswamy A, Ho OK, Kong AH, Sreenivasmurthy SG, Zhu Z, Su C, Liu J, Song J, Li M and Cheung KH (2022). Tetrandrine ameliorates cognitive deficits and mitigates tau aggregation in cell and animal models of tauopathies. *J. Biomed. Sci.*, **29**(1): 85.

Wang JW, Ye XY, Wei N, Wu SS, Zhang ZH, Luo GH, Li X, Li J and Cao H (2022). Reactive oxygen species contributes to type 2 diabetic neuropathic pain via the thioredoxin-interacting protein-NOD-like receptor protein 3- N -methyl-D-aspartic acid receptor 2B pathway. *Anesth. Analg.,* **135**(4): 865-876.

Wang XH, Lang R, Zeng Q, Liang Y, Chen N, Ma ZZ and Yu RH (2021). Jianpi Qushi Heluo formula alleviates renal damages in passive hemann nephritis in rats by upregulating parkin-mediated mitochondrial autophagy. *Sci. Rep.,* **11**(1): 18338.

Xu C, Jiang X, Yin W, Lyu L, Tan H, He W, Wang W, Zhou Z, Zhou H, Xu B, Yu Y, Wang Y, Zhou P, Liu Y, Xu J, Gou M and Hu Y (2025). Microgel-encapsulated tetrandrine nanoparticles promote spinal cord repair by sustaining neuroinflammation inhibition. *J. Mater. Chem. B.,* **13**(2): 683-694.

Yao H, Cai C, Huang W, Zhong C, Zhao T, Di J, Tang J, Wu D, Pang M, He L, Rong L and Liu B (2024).

Enhancing mitophagy by ligustilide through BNIP3-LC3 interaction attenuates oxidative stress-induced neuronal apoptosis in spinal cord injury. *Int. J. Biol. Sci.,* **20**(11): 4382-4406.

Yon DK, Kim YJ, Park DC, Jung SY, Kim SS, Yeo JH, Lee J, Lee JM and Yeo SG (2023). Induction of autophagy and its role in peripheral nerve regeneration after peripheral nerve injury. *Int. J. Mol. Sci.*, **24**(22): 16219.

Yuan H, Wang B, Ye Z and Li S (2023). Berberine alleviates the damage, oxidative stress and mitochondrial dysfunction of PC12 cells induced by high glucose by activating the KEAP1/Nrf2/ARE pathway. *Mol. Biotechnol.*, **65**(10): 1632-43.

Zhang ZL, Wang ZT, Shi J, Pu XP and Zhai SD (2023). Tetrandrine attenuates SNI-induced mechanical allodynia by inhibiting spinal CKLF1. *Neuropharmacology.,* **238**: 109673.

Zhang R, Lai M and Wang D (2022). Psychologic Impacts on diabetic neuropathic pain. *Curr. Pain. Headache. Rep.*, **26**(6): 423-27.

Zheng G, Ren J, Shang L and Bao Y (2023). Role of autophagy in the pathogenesis and regulation of pain. *Eur. J. Pharmacol.,* **955**: 175859.